## 4.3 Amplitude and Time Statistics

In order to determine system performance, more detailed statistical information about the received noise waveform is generally required than that given by $F_a$, $V_d$, and $L_d$. Some examples of such detailed statistics of the received waveform are given in this section.

Examples of the noise envelope amplitude probability distribution are given on figures 33-37. The APD's shown are plotted relative to the power moment (in dB relative to the rms envelope voltage). The APD shown in figure 33 was measured in a 4 kHz bandwidth and at a center frequency of 48 MHz. The measurement covered a 5-min period and was made at the intersection of 28th Street and Arapahoe, Boulder, Colorado, during the evening rush hour (1655-1700 LST). The level, because of the high traffic density at the time, is quite high, having been measured at 43.5 dB above $kT_o$. This is approximately 1 dB higher than the estimated upper decile value for business areas. The value of $V_d$ for this particular distribution is 5.4 dB. The APD's of the man-made radio noise measured at 102 MHz in a 4 kHz bandwidth at Grand Coulee Dam is shown on figure 34 and at Boulder, Colorado, on 30th Street between Walnut and Peak on figure 35. An APD measured in a rural area in the state of Washington is shown on figure 36. The absence of any nearby, high noise source precludes the occurrence of the very high noise spikes even at the 0.0001 percent point. The range of APD's given here for business areas (figs. 34 and 35) to rural (fig. 36) can be considered typical for this frequency and bandwidth.

The distributions measured along interstate 80 as shown on figure 37 exhibits considerably greater dynamic range than any of the other APD's shown. This principally is caused by the low rural background noise level with the high noise impulses from the traffic on the highway superimposed. This APD was measured at 48 MHz using a 10 kHz

bandwidth. The increase in bandwidth, 4 kHz to 10 kHz, will also increase the dynamic range of the noise envelope voltage.

The APD's are plotted on probability coordinates with an abscissa scale such that a Rayleigh distribution (the envelope distribution for a white Gaussian noise process) plots as a straight line with a slope of -1/2. The $V_{rms}$ level of a Rayleigh distribution is approximately at the 36 percent point. A Rayleigh envelope distribution for Gaussian noise is also shown on figure 33. Note that the lower amplitude, higher percentage portions of all the APD's are Rayleigh in character. Even the most impulsive noise will be composed of this Gaussian background with the high noise pulses superimposed upon it. Typical APD's and their variations for residential areas for 2.5, 10, 20, and 48 MHz and a 10-kHz bandwidth have been given by Spaulding et al. (1971).

The radio noise generated internal to the receiving system (antenna circuit losses, receiver noise, etc.) is Gaussian in character and will combine with the external noise. For all the distributions shown, the receiving system noise was well below the man-made noise level. That is, the internally generated noise had no effect on the measured distributions.

A number of 6-min analog tape recordings (see Appendix A) of the pre-detection noise process have been made. The recordings were detected (to obtain the noise envelope), digitized, and computer analyzed to obtain detailed envelope statistics.

Two examples of the analysis of these analog recordings are shown on figures 38-43 and figures 44-51. The first example is for a noise sample recorded in a 4 kHz bandwidth at 250 MHz. The recording was made in a business area in Colorado Springs, Colorado, June 5, 1970, 0857-0903 MST. A randomly selected 200 msec portion of the digitized envelope is shown on figure 38, while figure 39 shows the autocovariance for this 200 msec sample. Note that for short periods of time ($\tau < 100$ msec)

the noise appears to be uncorrelated. This is generally, but not always, the case. The APD for this 6-min recording is shown on figure 40. Also shown by the dashed Rayleigh distribution on figure 40 is the system (receiving, recording, playback, and digitizing) noise level. The average crossing rate characteristic (ACR) is shown on figure 41, while figures 42 and 43 show the pulse duration distributions (PDD) and the pulse spacing distributions (PSD), respectively.

The second example, also in a 4 kHz bandwidth, was recorded at 48 MHz in a Denver, Colorado, residential area. Two randomly selected 200 msec sample of the digitized envelope are shown on figures 44 and 46, and figures 45 and 47 give the corresponding autocovariance functions. Note the low level CW signal present on the second sample (figs. 46 and 47). The APD, ACR, PDD's, PSD's, for the 6-min recording are given on figures 48, 49, 50, and 51, respectively.

The average crossing rate, ACR, is the average number of positive crossings of given levels by the noise envelope. At the higher levels, a positive crossing of a level can be considered to correspond to the occurrence at the receiver input of a noise pulse of amplitude greater than that level. The maximum number of positive crossings depends on the receiver bandpass and noise characteristics. Additional ACR measurements have been given by ACLMRS (1966).

The pulse duration is the time that the noise pulse is above a particular envelope voltage level. That is, at a given level, it is the time between the positive crossing of the level and the next negative crossing. The curves on figures 42 and 50 show the percent (probability $\times$ 100) of pulses whose durations at the indicated level are equal to or greater than the time indicated by the ordinate.

The pulse spacing is the time from a negative crossing of a given level by the noise envelope to the next positive crossing of that level. The curves on figures 43 and 51 show the distribution of these times

for various levels. If man-made noise was composed of pulses occurring randomly according to a Poisson distribution, the pulse spacing distributions would be exponential at the higher envelope levels. An exponential distribution plots as a straight line of slope -1 on the coordinates used for figures 42, 43, 50, and 51. As can be seen from figures 43 and 51, the pulse spacing distributions at the higher levels and wider spacings are not exponential. This indicates correlation in the noise process for these longer time periods.

These samples of the various amplitude and time statistics given here are for guidance to provide some insight into the characteristics of the noise process. They are not, however, intended to be estimates of the statistics for all types of man-made radio noise. While these are examples of the statistics that will be found, they are not average values but strictly the results of the analysis of a few samples. The statistics for the various types of man-made radio noise encountered in the environment will vary with time, location, frequency, and the receiving system.

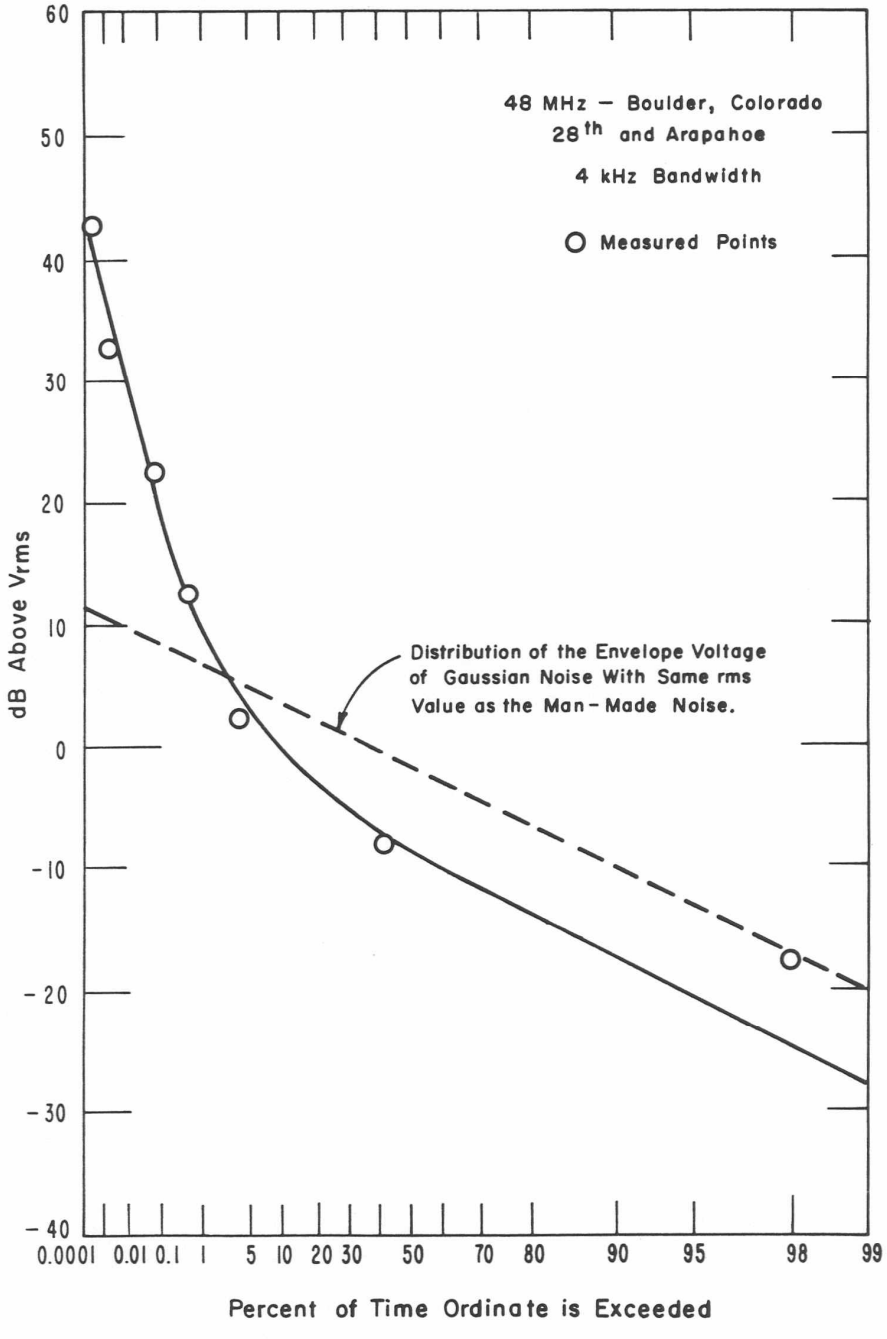


Figure 33. Amplitude probability distribution of envelope of man-made radio noise at 48 MHz.

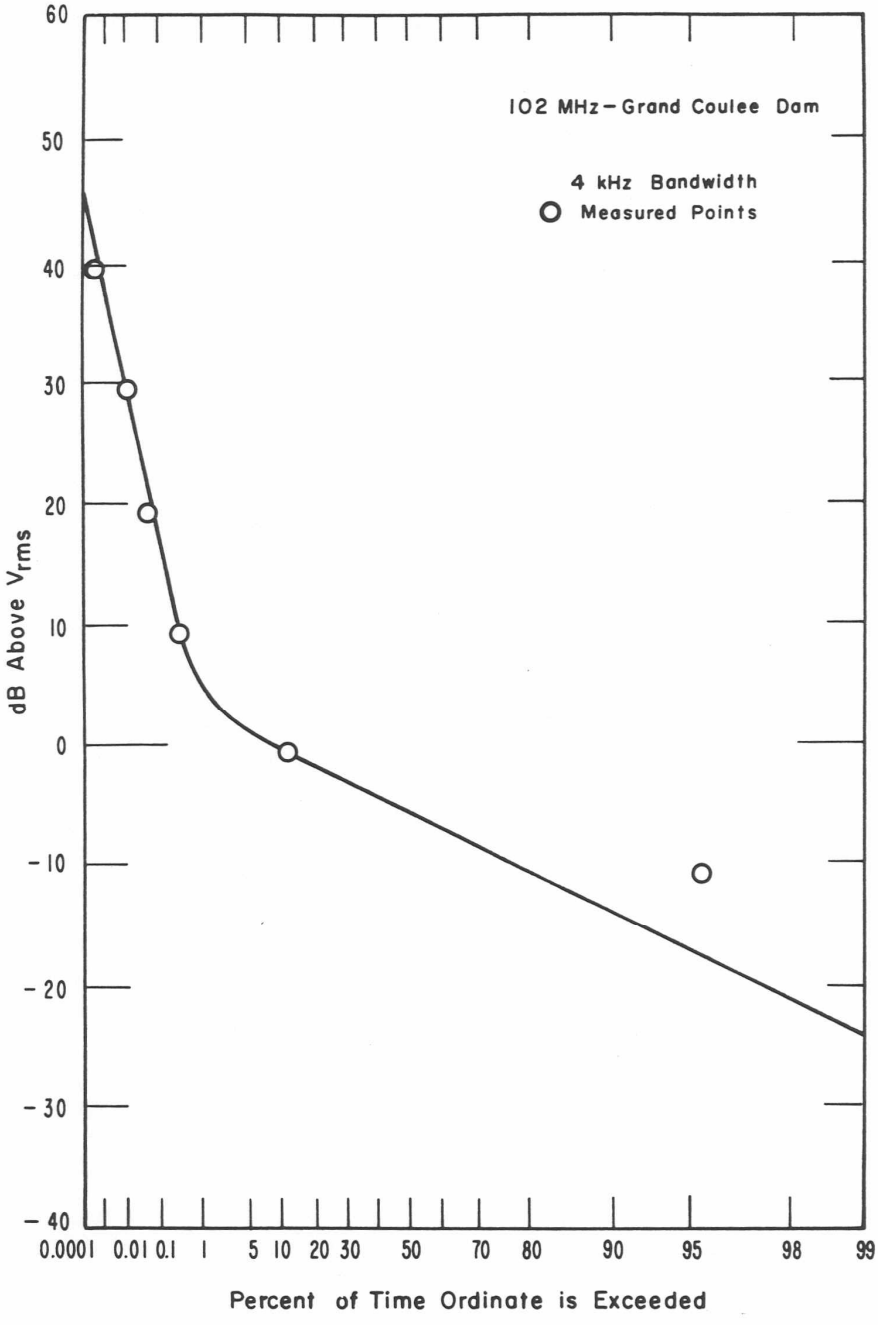


Figure 34. Amplitude probability distribution of man-made noise at 102 MHz.

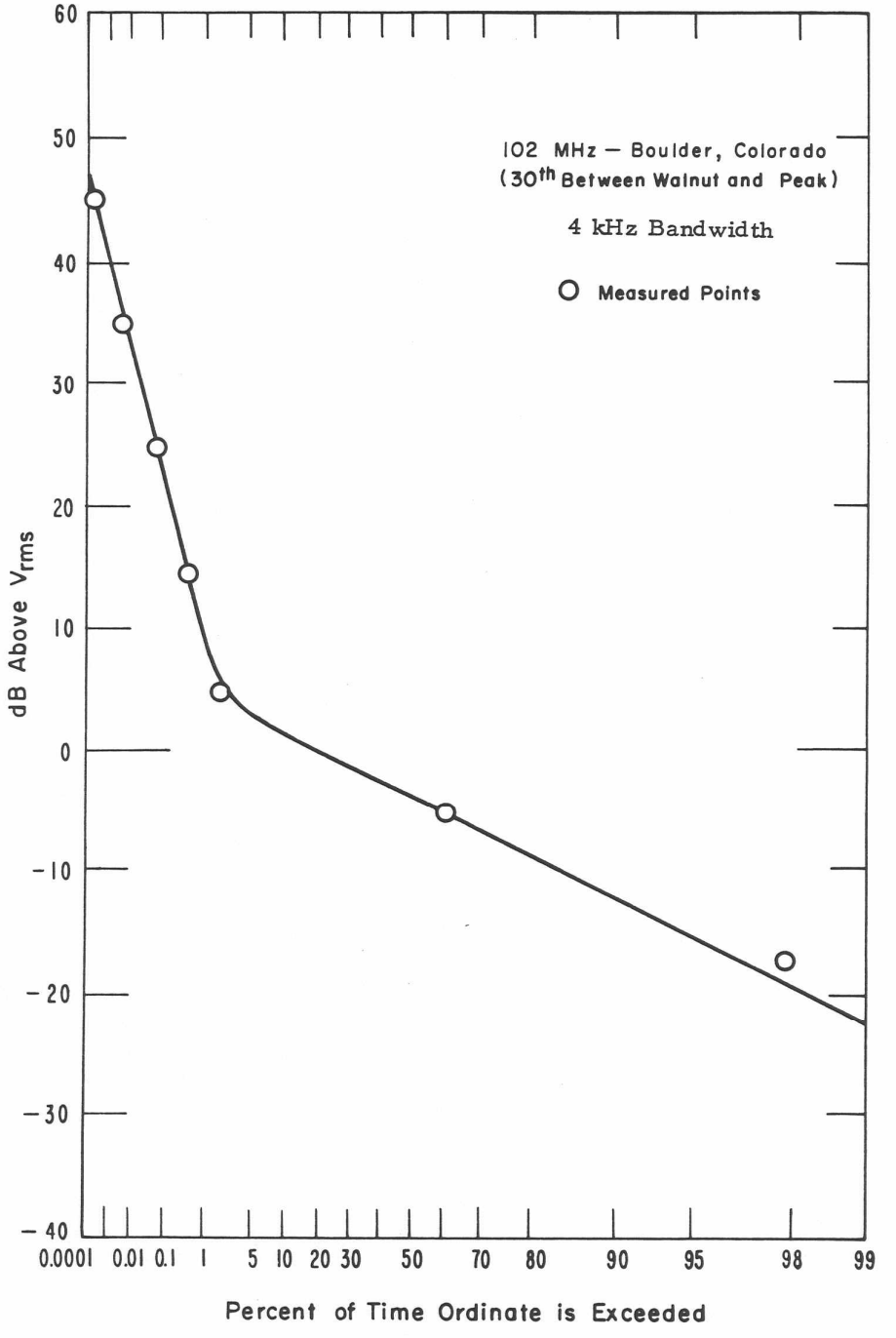


Figure 35. Amplitude probability distribution of man-made noise at 102 MHz.

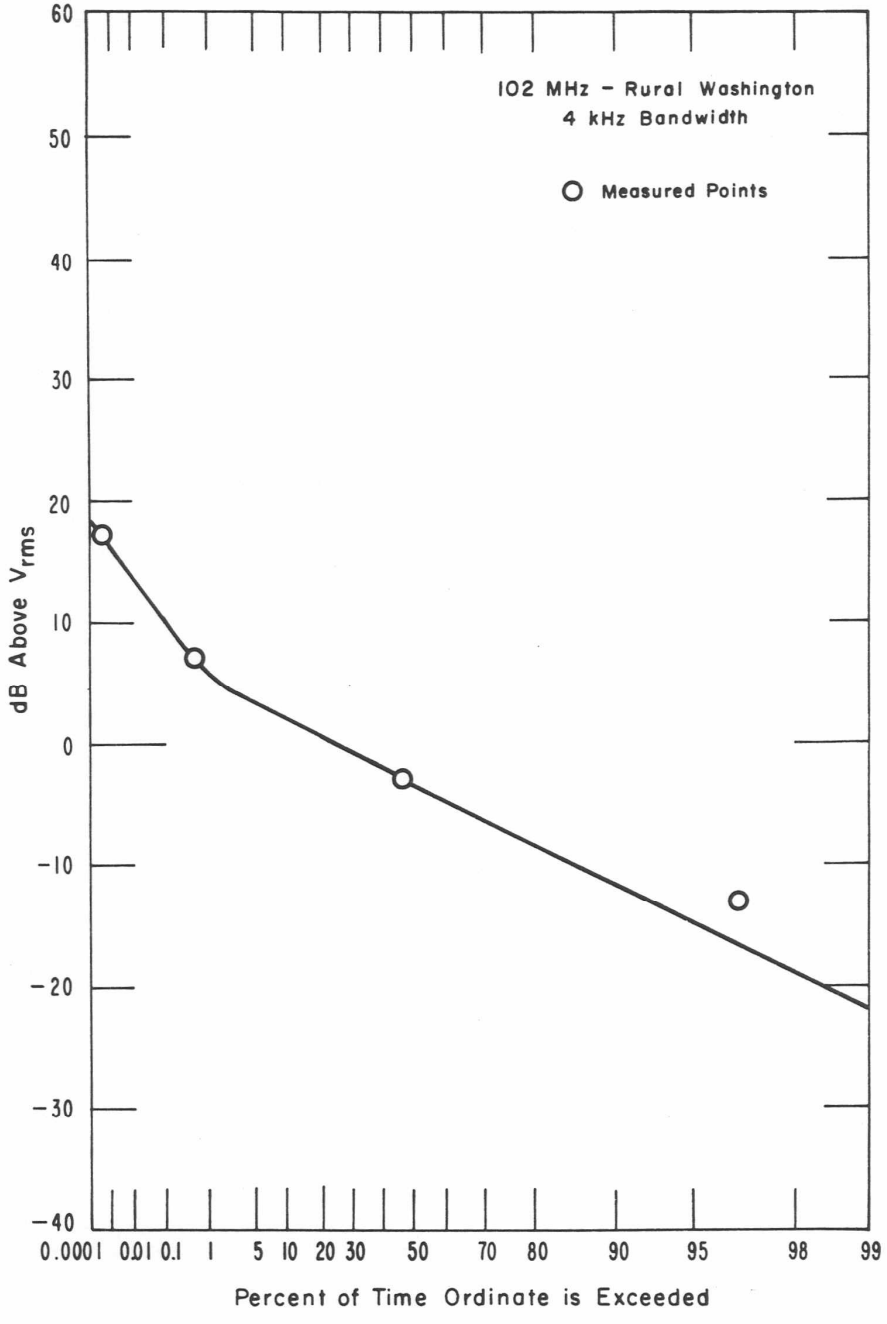


Figure 36. Amplitude probability distribution of man-made noise at 102 MHz.

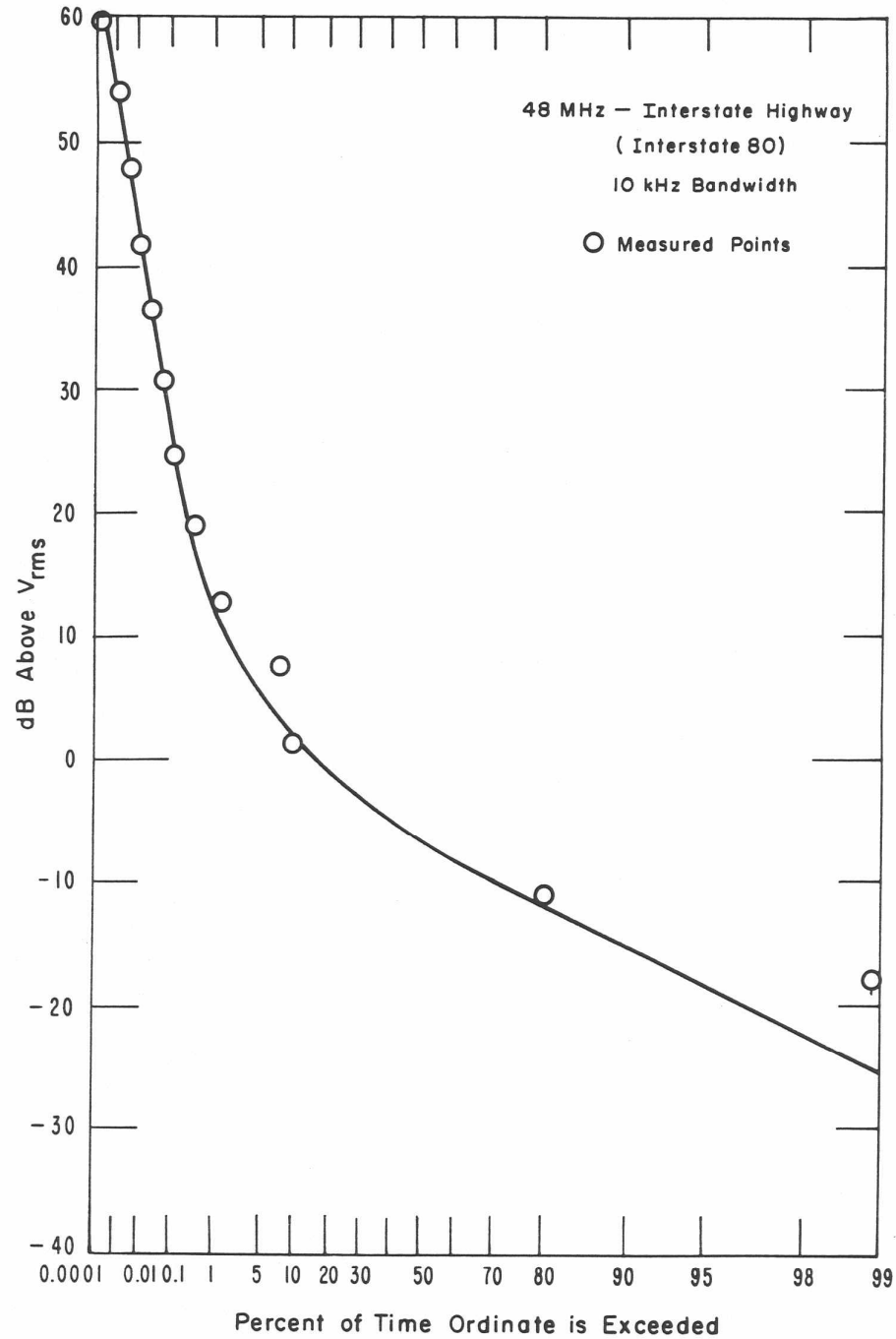


Figure 37. Amplitude probability distribution of man-made noise at 48 MHz, 10 kHz bandwidth.

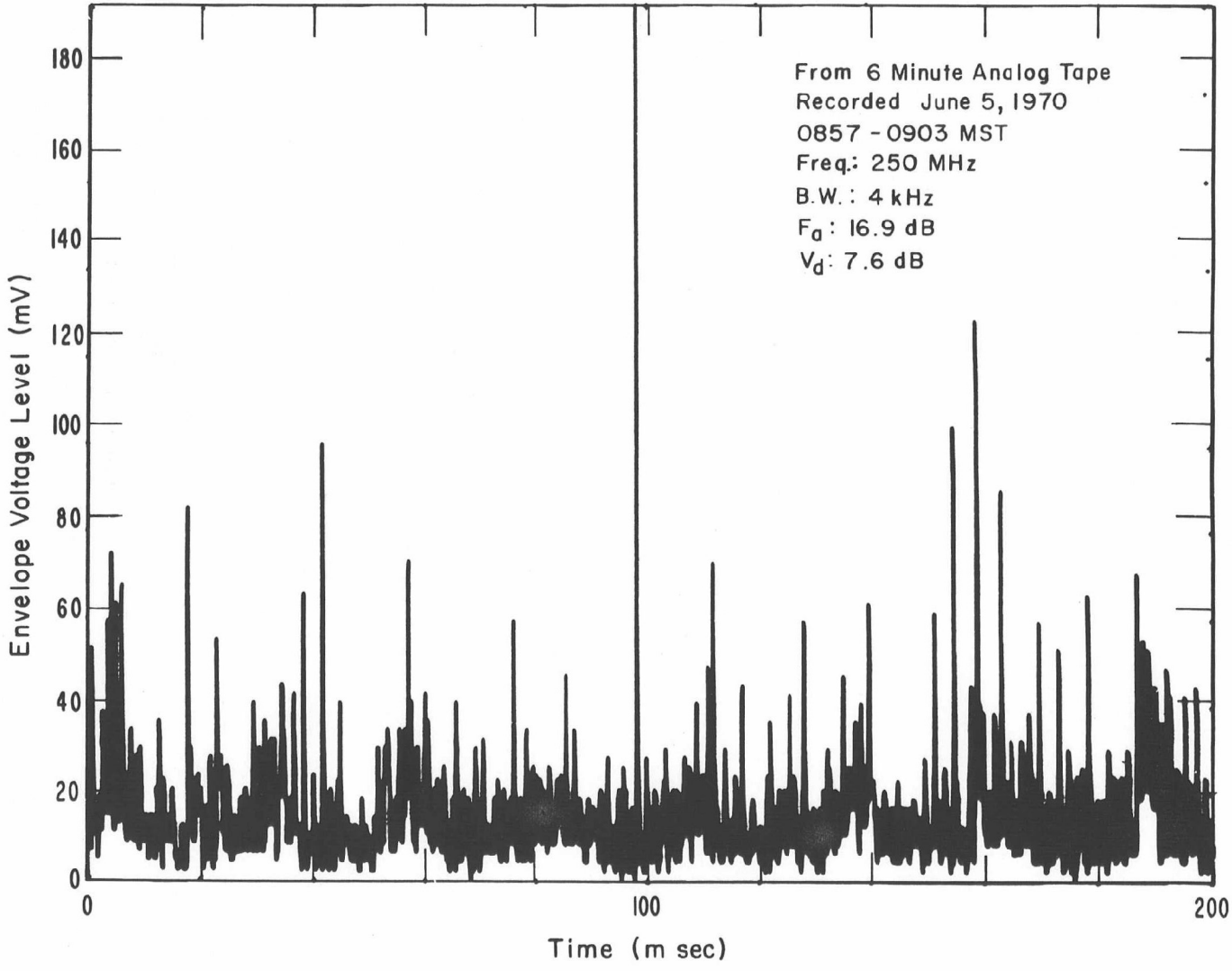


Figure 38. Randomly selected 200 ms sample of noise envelope from a 6-minute, 250 MHz central Colorado Springs recording.